Transmit Antenna Selection for Full-Duplex Spatial Modulation Multiple-Input Multiple-Output System

Le Van Nguyen, Ba Cao Nguyen, Xuan Nam Tran, *Member, IEEE*, and Le The Dung, *Member, IEEE*

***Abstract*—Transmit antenna selection (TAS) is an effective solution to enhance the performance of a multiple-input multiple-output (MIMO) system, especially when combined with spatial modulation (SM), and full duplex (FD) technique. However, there still lacks a comprehensive understanding on the system behavior of such a system. In this article, we consider a point-to-point bidirectional FD-SM-MIMO system using channel gain based TAS under the impact of imperfect successive interference cancellation and develop an analytical solution for analyzing its performance. In particular, we derive the exact closed-form expressions of the outage probability (OP) and the symbol error probability (SEP) for the FD-SM-MIMO system with TAS. The analytical solution can also be used for evaluating the performance of the half-duplex SM-MIMO (HD-SM-MIMO) systems with and without TAS. The OP, SEP, and system throughput of the FD-SM-MIMO system with TAS are evaluated against the case without using TAS and the HD-SM-MIMO system to demonstrate the benefits of using TAS and impact of the residual self-interference. All analysis results are validated by the Monte Carlo simulation ones to confirm the correctness of the derived mathematical expressions.**

***Index Terms*—Full-duplex (FD), multiple-input multiple-output (MIMO), outage probability (OP), self-interference cancellation (SIC), spatial modulation (SM), symbol error probability (SEP), transmit antenna selection (TAS).**

I. Introduction

THE world is witnessing the fast development of the fourth industrial revolution (aka. Industry 4.0), which can combine hardware, software, and biology into the so-called cyber-physical systems and emphasizes the advancements in communication and connectivity [1]. In such an era, the Internet of Things (IoT) plays an important role for providing connections for machine-to-machine networks. More bandwidths are expected to support the big data exchange.

Meanwhile, the cellular networks are also developing to the next generation, which can provide users with a higher access rate and more connection support. The fifth generation (5G) of mobile communications is expected to be officially released in 2020 to provide broadband access at low latency and high spectrum efficiency. It can also support massive machine type communications for IoT devices. In order for the 5G network to fulfill these requirements, various radio access technologies were considered for inclusion in its standards such as advanced modulation and coding, multiple-input multiple-output (MIMO), nonorthogonal multiple access, millimeter wave, and full-duplex (FD) [2]. Among these techniques, FD radio is a promising solution to attaining high spectrum efficiency as it allows for simultaneous transmission and reception at the same frequency, thereby theoretically doubling the network capacity. However, the FD radio systems are affected by the residual self-interference (RSI) at the FD devices due to the imperfect self-interference cancellation (SIC), which deteriorates the system performance [3]–[5]. Today, with the latest advancements in antenna design and signal processing, the FD devices can attain up to 110 dB SIC, thanks to the interference isolation, analog, and digital cancellation [6], [7], making the FD radio become more realistic.

Meanwhile, MIMO is an advanced antenna system, which can be used to achieve high channel capacity and high performance improvement, thanks to spatial diversity. MIMO transmission techniques such as space-time codes (STCs) and spatial multiplexing (SMX) have been used widely in the 3G and 4G systems. With their great advantages, STC and SMX are still the main radio transmission techniques for the 5G system. Following STC and SMX, spatial modulation (SM) is another MIMO transmission technique, which can achieve improved spectral efficiency but with lower complexity requirements in both hardware and signal processing compared with the former ones [8]. In the SM systems, the data bits are conveyed not only by the modulated symbols but also the indices of the active antennas. At a transmission interval, only one transmit antenna is activated, thereby avoiding the interchannel interference (ICI) and antenna synchronization problems. As such, only a radio frequency (RF) chain is required in the SM transmitter. Without ICI, the SM receiver can use maximal ratio combining (MRC) for diversity reception before jointly detecting the transmitted symbols and activated antenna. Various enhanced SM systems were proposed in the literature (see [9] and references therein).

In order to improve the system performance, Basar *et al.* [10] proposed to combine SM with the Alamouti's space-time block code (STBC) to attain the second-order diversity with low-complexity maximum likelihood (ML) detection. Using the

Manuscript received July 11, 2019; revised October 16, 2019; accepted December 12, 2019. *(Corresponding author: Le The Dung.)*

L. V. Nguyen and X. N. Tran are with Advanced Wireless Communications Group, Le Quy Don Technical University, Hanoi 10000, Vietnam (e-mail: nguyenlevan2211@gmail.com; namtx@mta.edu.vn).

B. C. Nguyen is with Advanced Wireless Communications Group, Le Quy Don Technical University, Hanoi 10000, Vietnam, and also with Telecommunications University, Nhatrang 650000, Vietnam (e-mail: nguyenbacao@tcu.edu.vn).

L. T. Dung is with the Division of Computational Physics, Institute for Computational Science, Ton Duc Thang University, Ho Chi Minh City 70000, Vietnam, and also with the Faculty of Electrical and Electronics Engineering, Ton Duc Thang University, Ho Chi Minh City 70000, Vietnam (e-mail: lethedung@tdtu.edu.vn).

Digital Object Identifier 10.1109/JSYST.2019.2960599

approach of spatial codeword design, Le *et al.* [11] proposed a spatially modulated orthogonal STBC scheme, which can achieve second-order diversity for an arbitrary number of transmit antennas and modulation order. Meanwhile, Di Renzo and Haas [12] proposed an SM-based transmit diversity scheme, which uses time-orthogonal shaping filters to attain the second-order diversity without reducing the transmission rate. Exploiting the cyclic structure and complex signal constellation rotation, another combined scheme of STBC and SM was proposed in [13], which can improve the spectral efficiency while still achieving the same diversity order. In a recent work, Tran *et al.* [14] proposed to combine the full-rate full-diversity golden code with SM to achieve the same second-order diversity but with higher spectral efficiency and less RF chains. In another approach, two antenna selection schemes based on Euclidean distance and capacity optimization were proposed for the SM system [15] to achieve the signal-to-noise ratio (SNR) gain for performance improvement. In a following work, Ntontin *et al.* [16] proposed an enhanced antenna subset selection scheme based on the Euclidean distance with low complexity. Using theoretical analysis, Kumbhani *et al.* [17] and [18] successfully derived the outage probability (OP) for the SM systems with antenna selection over the Rayleigh and Namagami-m channel, respectively.

In order to exploit the benefits of both FD radio and SM, different combinations of these techniques were considered in the literature [19]–[23]. In [19], Jiao *et al.* proposed an SM-FD system with adaptive SIC and investigated the instantaneous maximum mutual information in 2×2 MIMO system. In [19], Jiao *et al.* considered an FD-SM-MIMO system and derived the expressions of the OP and ergodic capacity for it. The symbol error probability (SEP) of this system under the impact of the RSI was derived. Besides OP and SEP, the bit error rate (BER) performance of the FD-SM-MIMO system was also analyzed in [22] and [23]. The cent work in [20] investigated an SM-MIMO system with FD amplify-and-forward (AF) relaying. The upper bound of BER was obtained for different modulation schemes. Taking into account the direct link from source to destination, Narayanan *et al.* [21] analyzed an FD-SM-MIMO system whose relay uses both AF and decode-and-forward protocols.

Although the FD-SM-MIMO system has been widely studied in the literature, the advantage of transmit antenna selection (TAS) has not been considered yet. Furthermore, due to the presence of the RSI, the analysis results obtained for the HD-SM-MIMO system with TAS, such as in [17] and [18], are not applicable for the FD-SM-MIMO system. Motivated by these issues, in this article, we consider an FD-SM-MIMO system with TAS and conduct a detailed performance analysis to gain an insight into its operation. Specifically, we derive the exact closed-form expressions of the OP and SEP for the FD-SM-MIMO system with TAS based on the channel gain selection. The main contributions of this article can be summarized as follows.

1) We investigate a point-to-point bidirectional FD-SM-MIMO system with TAS based on channel gain selection and analyze its performance under the impact of the RSI at both terminals over the Rayleigh fading channel.

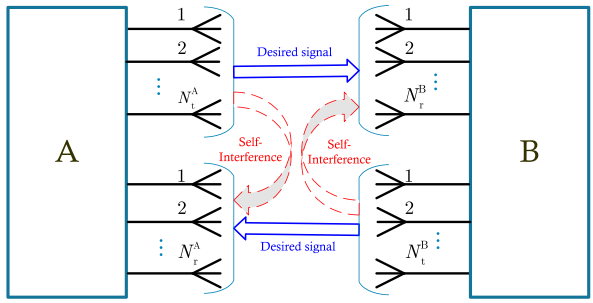

Fig. 1. System model of the considered FD-SM-MIMO system with self-interference.

2) We develop an analytical solution with the exact expressions of the OP and SEP for the FD-SM-MIMO system in the case with and without using TAS. Our solution can also be used for analyzing the HD-SM-MIMO system with and without TAS.
3) Using the analytical solution, key performance measures such as the OP, network throughput, and SEP of the FD-SM-MIMO system are compared with those of the HD-SM-MIMO system under the impacts of the RSI and the number of transceiver antennas.

The rest of the article is organized as follows. Section II presents the system models of the FD-SM-MIMO system under consideration. Section III focuses on the derivations of the exact closed-form expressions of the OP and SEP. Numerical results and discussion are given in Section IV. Finally, Section V draws the conclusion of the article.

II. System Model

We consider an FD-SM-MIMO system with TAS as illustrated in Fig. 1. The information data are exchanged between two communication terminals, A and B. Both A and B are MIMO devices which operate in the FD mode with separate transmit and receive antennas. Specifically, A and B have $N_{\rm t}^{\rm A}$, $N_{\rm t}^{\rm B}$ antennas for transmission and $N_{\rm r}^{\rm A}$, $N_{\rm r}^{\rm B}$ antennas for reception, respectively. In some certain systems, A and B can use shared antennas to transmit and receive signals simultaneously in order to reduce the system complexity. However, using the two separate antennas as in our system provides better self-interference (SI) suppression [6], [24]. As shown in Fig. 1, when A and B operate in the FD mode, the SI from transmission antennas to reception antennas will distort the quality of the desired signals.

At time slot t, the received signal at A and B are, respectively, given by

$$\mathbf{y}_{\rm A}(t) = \sqrt{P_{\rm B}}\mathbf{h}_j^{\rm A} x_j(t) + \sqrt{P}_{\rm A}\mathbf{h}_i^{\rm A} x_i(t) + \mathbf{z}_{\rm A}(t) \quad (1)$$

$$\mathbf{y}_{\rm B}(t) = \sqrt{P_{\rm A}}\mathbf{h}_i^{\rm B} x_i(t) + \sqrt{P}_{\rm B}\mathbf{h}_j^{\rm B} x_j(t) + \mathbf{z}_{\rm B}(t) \quad (2)$$

where $x_i(t)$ and $x_j(t)$ are the transmitted signals from the ith antenna of A and the jth antenna of B, respectively; $P_{\rm A}$ and $P_{\rm B}$ are the average transmission power of A and B, respectively; $\mathbf{h}_i^{\rm B}$ and $\mathbf{h}_j^{\rm A}$ denote the coefficient vector of the channel from the ith transmission antenna of A to $N_{\rm r}^{\rm B}$ reception antennas of B and from the jth transmission antenna of B to $N_{\rm r}^{\rm A}$ reception antennas

of A, respectively; $\mathbf{h}_i^{\mathrm{A}}$ and $\mathbf{h}_j^{\mathrm{B}}$ are, respectively, the SI channel coefficient vectors reflecting the effect of transmission leakage from the ith transmission antenna to $N_{\mathrm{r}}^{\mathrm{A}}$ reception antennas of A and from the jth transmission antenna to $N_{\mathrm{r}}^{\mathrm{B}}$ reception antennas of B; $\mathbf{z}_{\mathrm{A}}(t)$ and $\mathbf{z}_{\mathrm{B}}(t)$ are, respectively, the additive white Gaussian noise (AWGN) vector at A and B, whose elements have zero mean and variance of σ^2, i.e., $\mathbf{z}_{\mathrm{A}} \sim C\mathcal{N}(0, \sigma_{\mathrm{A}}^2)$ and $\mathbf{z}_{\mathrm{B}} \sim C\mathcal{N}(0, \sigma_{\mathrm{B}}^2)$. It is also noted that $\mathbf{h}_j^{\mathrm{A}}$ and $\mathbf{h}_i^{\mathrm{B}}$ are defined as follows:

$$\mathbf{h}_j^{\mathrm{A}} = \left[h_{j1}\ h_{j2}\ \ldots\ h_{jN_{\mathrm{r}}^{\mathrm{A}}}\right] \tag{3}$$

$$\mathbf{h}_i^{\mathrm{B}} = \left[h_{i1}\ h_{i2}\ \ldots\ h_{iN_{\mathrm{r}}^{\mathrm{B}}}\right] \tag{4}$$

where $i = 1, 2, \ldots, N_{\mathrm{t}}^{\mathrm{A}}$ and $j = 1, 2, \ldots, N_{\mathrm{t}}^{\mathrm{B}}$.

Since the space between the transmission to the reception antenna of each terminal is limited, the SI power is stronger than that of the desired signal. Hence, all SIC available techniques in the propagation, digital and analog domain [6], [7] need to be applied for the best SI suppression. Thanks to the separate antennas for signal transmission and reception, A and B can use advanced interference isolation techniques in the propagation domain to reduce better the SI leakage. After all the SIC processing, the RSI at A and B, respectively denoted by $\mathbf{r}_{\mathrm{SI_A}}$ and $\mathbf{r}_{\mathrm{SI_B}}$, become small and are often modeled by complex Gaussian random variables with zero mean and variances σ_{RSI}^2, i.e., $\sigma_{\mathrm{RSI_A}}^2 = \tilde{\Omega}_{\mathrm{A}} P_{\mathrm{A}}$ and $\sigma_{\mathrm{RSI_B}}^2 = \tilde{\Omega}_{\mathrm{B}} P_{\mathrm{B}}$ [25]–[30]. Here, $\tilde{\Omega}_{\mathrm{A}}$ and $\tilde{\Omega}_{\mathrm{B}}$ indicate the SIC capability of A and B, respectively.

Under the above assumptions, the received signals at A and B after SIC are given by

$$\mathbf{y}_{\mathrm{A}}(t) = \sqrt{P_{\mathrm{B}}}\mathbf{h}_j^{\mathrm{A}} x_j(t) + \mathbf{r}_{\mathrm{SI_A}}(t) + \mathbf{z}_{\mathrm{A}}(t) \tag{5}$$

$$\mathbf{y}_{\mathrm{B}}(t) = \sqrt{P_{\mathrm{A}}}\mathbf{h}_i^{\mathrm{B}} x_i(t) + \mathbf{r}_{\mathrm{SI_B}}(t) + \mathbf{z}_{\mathrm{B}}(t). \tag{6}$$

In the conventional FD-SM-MIMO system, only one antenna is chosen from $N_{\mathrm{t}}^{\mathrm{A}}$ transmission antenna of A and only one antenna is chosen from $N_{\mathrm{t}}^{\mathrm{B}}$ transmission antenna of B. However, in the case with TAS, a set of only S_{A} antennas are selected from $N_{\mathrm{t}}^{\mathrm{A}}$ transmission antennas of A and a set of only S_{B} antennas are selected from $N_{\mathrm{t}}^{\mathrm{B}}$ transmission antennas for performance improvement. It is worth noting that S_{A} and S_{B} are subject to $S_{\mathrm{A}} = 2^m \leq N_{\mathrm{t}}^{\mathrm{A}}$, and $S_{\mathrm{B}} = 2^n \leq N_{\mathrm{t}}^{\mathrm{B}}$ with m and n being positive integers. The selected sets S_{A} and S_{B} are chosen such that the total received signal power is maximized. For example, when the norms of the channel coefficients satisfy

$$\|\mathbf{h}_{1\mathrm{B}}\|^2 \geq \|\mathbf{h}_{2\mathrm{B}}\|^2 \geq \|\mathbf{h}_{3\mathrm{B}}\|^2 \geq \cdots \geq \|\mathbf{h}_{N_{\mathrm{t}}^{\mathrm{A}}\mathrm{B}}\|^2 \tag{7}$$

and $|S_{\mathrm{A}}| = 2$, we have the set S_{A} as follows:

$$S_{\mathrm{A}} = \{\|\mathbf{h}_{1\mathrm{B}}\|^2, \|\mathbf{h}_{2\mathrm{B}}\|^2\}. \tag{8}$$

From this set, depending on the transmitted data bits, either the first or the second antenna of A is activated. At the receiver side, the MRC is used to coherently combine the signals from N_{r} reception antennas ($N_{\mathrm{r}}^{\mathrm{A}}$ at terminal A and $N_{\mathrm{r}}^{\mathrm{B}}$ at terminal B). Then, in order to recover the transmitted bits, the receiver can use the joint ML detection for estimating both the activated transmit antenna index and the M-ary modulated symbols. In this article, as we are interested in analyzing the impact of the RSI due to the FD mode as well as the effect of the TAS scheme on the system performance, we assume that the receivers of both A and B can perfectly estimate the activated antenna indices of the respective transmitters for the ML detection [30]–[32].

Based on the system equations in (5) and (6), the signal-to-inteference-plus-noise ratio (SINR) at terminal A (denoted by γ_{A}) and terminal B (denoted by γ_{B}) can be given by

$$\gamma_{\mathrm{A}} = \frac{\|\mathbf{h}_j^{\mathrm{A}}\|^2 P_{\mathrm{B}}}{\sigma_{\mathrm{RSI_A}}^2 + \sigma_{\mathrm{A}}^2} = \|\mathbf{h}_j^{\mathrm{A}}\|^2 \bar{\gamma}_{\mathrm{A}} \tag{9}$$

$$\gamma_{\mathrm{B}} = \frac{\|\mathbf{h}_i^{\mathrm{B}}\|^2 P_{\mathrm{A}}}{\sigma_{\mathrm{RSI_B}}^2 + \sigma_{\mathrm{B}}^2} = \|\mathbf{h}_i^{\mathrm{B}}\|^2 \bar{\gamma}_{\mathrm{B}} \tag{10}$$

where

$$\bar{\gamma}_{\mathrm{A}} = \frac{P_{\mathrm{B}}}{\sigma_{\mathrm{RSI_A}}^2 + \sigma_{\mathrm{A}}^2}, \text{ and } \bar{\gamma}_{\mathrm{B}} = \frac{P_{\mathrm{A}}}{\sigma_{\mathrm{RSI_B}}^2 + \sigma_{\mathrm{B}}^2}$$

are, respectively, the average SINRs at terminals A and B.

III. Performance Analysis

In this section, we derive the exact closed-form expression for the OP and, then, obtain the SEP of the FD-SM-MIMO system. Since the SINRs at A and B are similar, we will present only the detailed derivations for the OP and SEP of B. These expressions of A can be obtained in the same way.

A. Outage Probability

For the considered FD-SM-MIMO system, the data bits are conveyed not only by the modulated symbol but also by the index of the activated antenna element. Therefore, the data rate of the considered system can be calculated as [30]–[32]

$$\mathcal{R}_{\mathrm{SM}} = \log_2(N_{\mathrm{t}}) + \log_2(1 + \gamma) \tag{11}$$

where N_t is the number of transmission antennas ($N_{\mathrm{t}}^{\mathrm{A}}$ at terminal A and $N_{\mathrm{t}}^{\mathrm{B}}$ at terminal B); and γ is the SINR at the receiver (γ_{A} at terminal A and γ_{B} at terminal B). It is noted that the term $\log_2(N_{\mathrm{t}})$ denotes the capacity obtained by the SM technique.

In the case of perfect estimation of antenna index, the OP at terminal B is defined as [30]–[32]

$$\mathcal{P}_{\mathrm{out}}^{\mathrm{B}} = \Pr\{\log_2(N_{\mathrm{t}}^{\mathrm{A}}) + \log_2(1 + \gamma_{\mathrm{B}}) < \mathcal{R}_0\} \tag{12}$$

where γ_{B} is given in (10), $\mathcal{R}_0$ is the data transmission rate of the link from A to B, the term $\log_2(N_{\mathrm{t}}^{\mathrm{A}})$ denotes the number of bits, which are used for activating the transmission antenna at the transmitter A.

Replacing γ_{B} in (10) into (12), we can rewrite (12) as

$$\mathcal{P}_{\mathrm{out}}^{\mathrm{B}} = \Pr\{\gamma_{\mathrm{B}} < 2^{\mathcal{R}} - 1\} = \Pr\left\{\|\mathbf{h}_i^{\mathrm{B}}\|^2 < \frac{2^{\mathcal{R}} - 1}{\bar{\gamma}_{\mathrm{B}}}\right\} \tag{13}$$

where $\mathcal{R} = \mathcal{R}_0 - \log_2(N_{\mathrm{t}}^{\mathrm{A}})$ is the data rate obtained by the modulation scheme.

Denote the threshold $\gamma_{\mathrm{th}} = 2^{\mathcal{R}} - 1$, then the probability in (13) becomes

$$\mathcal{P}_{\mathrm{out}}^{\mathrm{B}} = \Pr\left\{\|\mathbf{h}_i^{\mathrm{B}}\|^2 < \frac{\gamma_{\mathrm{th}}}{\bar{\gamma}_{\mathrm{B}}}\right\}. \tag{14}$$

From (14), we obtain the OP of the FD-SM-MIMO system in Theorem 1 below.

Theorem 1: The OPs of terminal A (denoted by $\mathcal{P}_{\text{out}}^{\text{A}}$) and terminal B (denoted by $\mathcal{P}_{\text{out}}^{\text{B}}$) in the FD-SM-MIMO system with TAS over the Rayleigh fading channel are given by

$$\mathcal{P}_{\text{out}}^{\text{A}} = \frac{\pi\gamma_{\text{th}}}{2M(N_{\text{t}}^{\text{B}} - w_{\text{B}} + 1)\Gamma(N_{\text{r}}^{\text{A}})\bar{\gamma}_{\text{A}}} \times \sum_{l=w_{\text{B}}}^{N_{\text{t}}^{\text{B}}} \sum_{m=1}^{M} \frac{\sqrt{1-\phi_m^2}}{B(l, N_{\text{t}}^{\text{B}} - l + 1)} \left[1 - \frac{\Gamma(N_{\text{r}}^{\text{A}}, \chi_{\text{A}})}{\Gamma(N_{\text{r}}^{\text{A}})}\right]^{l-1} \times \left[\frac{\Gamma(N_{\text{r}}^{\text{A}}, \chi_{\text{A}})}{\Gamma(N_{\text{r}}^{\text{A}})}\right]^{N_{\text{t}}^{\text{B}}-l} \chi_{\text{A}}^{N_{\text{r}}^{\text{A}}-1} e^{-\chi_{\text{A}}} \tag{15}$$

$$\mathcal{P}_{\text{out}}^{\text{B}} = \frac{\pi\gamma_{\text{th}}}{2M(N_{\text{t}}^{\text{A}} - w_{\text{A}} + 1)\Gamma(N_{\text{r}}^{\text{B}})\bar{\gamma}_{\text{B}}} \times \sum_{l=w_{\text{A}}}^{N_{\text{t}}^{\text{A}}} \sum_{m=1}^{M} \frac{\sqrt{1-\phi_m^2}}{B(l, N_{\text{t}}^{\text{A}} - l + 1)} \left[1 - \frac{\Gamma(N_{\text{r}}^{\text{B}}, \chi_{\text{B}})}{\Gamma(N_{\text{r}}^{\text{B}})}\right]^{l-1} \times \left[\frac{\Gamma(N_{\text{r}}^{\text{B}}, \chi_{\text{B}})}{\Gamma(N_{\text{r}}^{\text{B}})}\right]^{N_{\text{t}}^{\text{A}}-l} \chi_{\text{B}}^{N_{\text{r}}^{\text{B}}-1} e^{-\chi_{\text{B}}} \tag{16}$$

where $\chi_{\text{A}} = \frac{\gamma_{\text{th}}}{2\bar{\gamma}_{\text{A}}}(1+\phi_m); \chi_{\text{B}} = \frac{\gamma_{\text{th}}}{2\bar{\gamma}_{\text{B}}}(1+\phi_m); w_{\text{A}} = N_{\text{t}}^{\text{A}} - S_{\text{A}} + 1; w_{\text{B}} = N_{\text{t}}^{\text{B}} - S_{\text{B}} + 1$; $B(.,.)$, $\Gamma(.)$ and $\Gamma(.,.)$ are the beta, gamma, and incomplete gamma functions [33], respectively; M is the complexity-accuracy tradeoff parameter; $\phi_m = \cos(\frac{(2m-1)\pi}{2M})$.

Proof: To derive the closed-form expression for the OP of A and B, we start with the cumulative distribution function (CDF) and the probability density function (PDF) of a random instantaneous channel gain $|h|^2$, which follows the Rayleigh fading distribution. Specifically, the CDF and PDF of $|h|^2$ are given by

$$F_{|h|^2}(x) = \Pr\{|h|^2 < x\} = 1 - e^{-\frac{x}{\Omega}}, x \geqslant 0 \tag{17}$$

$$f_{|h|^2}(x) = \frac{1}{\Omega} e^{-\frac{x}{\Omega}}, x \geqslant 0 \tag{18}$$

where $\Omega = \mathbb{E}\{|h|^2\}$ is the average channel gain of $|h|^2$. For the derivation convenience, we set $\Omega = 1$. For the summation of N_{r} channel gains, such as $Y = \|\mathbf{h}_i^{\text{B}}\|^2 = \sum_{l=1}^{N_{\text{r}}^{\text{B}}} |h_{il}|^2$, its PDF and CDF are expressed, respectively, as follows [3]:

$$F_Y(x) = 1 - e^{-x} \sum_{l=0}^{N_{\text{r}}^{\text{B}}-1} \frac{x^l}{l!}, \quad x \geq 0 \tag{19}$$

$$f_Y(x) = \frac{x^{N_{\text{r}}^{\text{B}}-1} e^{-x}}{\Gamma(N_{\text{r}}^{\text{B}})}, \quad x \geq 0. \tag{20}$$

■

Based on the above equations and combining with the Gaussian–Chebyshev quadrature method in [34], we can obtain the OPs of terminals A and B in the FD-SM-MIMO system in Theorem 1. The detailed proofs are presented in Appendix A.

It is also noted that in the case without TAS, based on (19), the OPs of the FD-SM-MIMO system are given by

$$\mathcal{P}_{\text{out,no-TAS}}^{\text{A}} = 1 - e^{-\frac{\gamma_{\text{th}}}{\bar{\gamma}_{\text{A}}}} \sum_{l=0}^{N_{\text{r}}^{\text{A}}-1} \frac{\left(\frac{\gamma_{\text{th}}}{\bar{\gamma}_{\text{A}}}\right)^l}{l!} \tag{21}$$

$$\mathcal{P}_{\text{out,no-TAS}}^{\text{B}} = 1 - e^{-\frac{\gamma_{\text{th}}}{\bar{\gamma}_{\text{B}}}} \sum_{l=0}^{N_{\text{r}}^{\text{B}}-1} \frac{\left(\frac{\gamma_{\text{th}}}{\bar{\gamma}_{\text{B}}}\right)^l}{l!}. \tag{22}$$

B. Symbol Error Probability

For a wireless system, the SEP can be calculated as [35]

$$\text{SEP} = a\mathbb{E}\left\{Q(\sqrt{b\gamma})\right\} = \frac{a}{\sqrt{2\pi}} \int_0^{\infty} F\left(\frac{t^2}{b}\right) e^{-\frac{t^2}{2}} dt \tag{23}$$

where $Q(x)$ denotes the Gaussian function; γ is the SINR; a and b are constants and their values are decided by the modulation types, e.g., $a = 1, b = 2$ for the binary phase-shift keying (BPSK) modulation; $a = 2, b = 1$ for the 4-quadrature amplitude modulation [35]; and $F(x)$ is the CDF of the SINR. Let $x = \frac{t^2}{b}$, then (23) becomes

$$\text{SEP} = \frac{a\sqrt{b}}{2\sqrt{2\pi}} \int_0^{\infty} \frac{e^{-bx/2}}{\sqrt{x}} F(x) dx. \tag{24}$$

From (24), we can derive the SEP of the FD-SM-MIMO system in Theorem 2 given below.

Theorem 2: The SEPs of terminal A (denoted by SEP_{A}) and terminal B (denoted by SEP_{B}) in the FD-SM-MIMO system with TAS over Rayleigh fading channel are given, respectively, as follows:

$$\text{SEP}_{\text{A}} = \frac{a\sqrt{b\pi^3}}{8\sqrt{2}MN(N_{\text{t}}^{\text{B}} - w_{\text{B}} + 1)\Gamma(N_{\text{r}}^{\text{A}})\bar{\gamma}_{\text{A}}} \times \sum_{l=w_{\text{B}}}^{N_{\text{t}}^{\text{B}}} \sum_{m=1}^{M} \sum_{n=1}^{N} \frac{\sqrt{(1-\phi_m^2)(1-\phi_n^2)}\psi_{\text{A}}^{N_{\text{r}}^{\text{A}}-1}}{(\psi_{\text{A}} + \frac{b}{2})B(l, N_{\text{t}}^{\text{B}} - l + 1)} \times \left[1 - \frac{\Gamma\left(N_{\text{r}}^{\text{A}}, \frac{-\psi_{\text{A}} \ln v}{\psi_{\text{A}} + \frac{b}{2}}\right)}{\Gamma(N_{\text{r}}^{\text{A}})}\right]^{l-1} \times \left[\frac{\Gamma\left(N_{\text{r}}^{\text{A}}, \frac{-\psi_{\text{A}} \ln v}{\psi_{\text{A}} + \frac{b}{2}}\right)}{\Gamma(N_{\text{r}}^{\text{A}})}\right]^{N_{\text{t}}^{\text{B}}-l} \left(\frac{-\ln v}{\psi_{\text{A}} + \frac{b}{2}}\right)^{N_{\text{r}}^{\text{A}} - \frac{1}{2}} \tag{25}$$

$$\text{SEP}_{\text{B}} = \frac{a\sqrt{b\pi^3}}{8\sqrt{2}MN(N_{\text{t}}^{\text{A}} - w_{\text{A}} + 1)\Gamma(N_{\text{r}}^{\text{B}})\bar{\gamma}_{\text{B}}} \times \sum_{l=w_{\text{A}}}^{N_{\text{t}}^{\text{A}}} \sum_{m=1}^{M} \sum_{n=1}^{N} \frac{\sqrt{(1-\phi_m^2)(1-\phi_n^2)}\psi_{\text{B}}^{N_{\text{r}}^{\text{B}}-1}}{(\psi_{\text{B}} + \frac{b}{2})B(l, N_{\text{t}}^{\text{A}} - l + 1)} \times \left[1 - \frac{\Gamma\left(N_{\text{r}}^{\text{B}}, \frac{-\psi_{\text{B}} \ln v}{\psi_{\text{B}} + \frac{b}{2}}\right)}{\Gamma(N_{\text{r}}^{\text{B}})}\right]^{l-1} \times \left[\frac{\Gamma\left(N_{\text{r}}^{\text{B}}, \frac{-\psi_{\text{B}} \ln v}{\psi_{\text{B}} + \frac{b}{2}}\right)}{\Gamma(N_{\text{r}}^{\text{B}})}\right]^{N_{\text{t}}^{\text{A}}-l} \left(\frac{-\ln v}{\psi_{\text{B}} + \frac{b}{2}}\right)^{N_{\text{r}}^{\text{B}} - \frac{1}{2}} \tag{26}$$

where N is the complexity-accuracy tradeoff parameter; $\phi_n = \cos(\frac{(2n-1)\pi}{2N})$; $\psi_{\rm A} = \frac{1}{2\bar{\gamma}_{\rm A}}(1+\phi_m)$; $\psi_{\rm B} = \frac{1}{2\bar{\gamma}_{\rm B}}(1+\phi_m)$; $v = \frac{1}{2}(1+\phi_n)$.

Proof: To calculate ${\rm SEP}_{\rm B}$, we start with the definition of the CDF of the SINR at terminal B, i.e.,

$$F_{\gamma_{\rm B}}(x) = \Pr\{\gamma_{\rm B} < x\} = \Pr\left\{\|\mathbf{h}_i^{\rm B}\|^2 < \frac{x}{\bar{\gamma}_{\rm B}}\right\}. \quad (27)$$

■

We can obtain this CDF by replacing $\gamma_{\rm th}$ in the OP expression given in (14) by x. Then, we substitute $F_{\gamma_{\rm B}}(x)$ into (24) to compute ${\rm SEP}_{\rm B}$. After some mathematical transforms and applying the Gaussian–Chebyshev quadrature method in [34], we obtain ${\rm SEP}_{\rm B}$ as in (26). The expression of ${\rm SEP}_{\rm A}$ can be obtained similarly. For detailed proofs, see in Appendix B.

In the case without TAS, replacing the OPs in (21) and (22) into (24), and then applying [34, Eq. 3.361.2] and [34, Eq. 3.381.4], we have

$${\rm SEP}_{\rm A,no-TAS} = \frac{a}{2} - \frac{a\sqrt{b}}{2\sqrt{2\pi}} \sum_{l=0}^{N_{r\rm A}-1} \frac{2^l \sqrt{2\bar{\gamma}_{\rm A}}\Gamma(l+\frac{1}{2})}{l!(2+\bar{\gamma}_{\rm A}b)^{(l+\frac{1}{2})}} \quad (28)$$

$${\rm SEP}_{\rm B,no-TAS} = \frac{a}{2} - \frac{a\sqrt{b}}{2\sqrt{2\pi}} \sum_{l=0}^{N_{r\rm B}-1} \frac{2^l \sqrt{2\bar{\gamma}_{\rm B}}\Gamma(l+\frac{1}{2})}{l!(2+\bar{\gamma}_{\rm B}b)^{(l+\frac{1}{2})}}. \quad (29)$$

IV. Numerical Results and Discussions

In this section, we evaluate the performance of the FD-SM-MIMO system with TAS and compare it with that of the system without TAS. Moreover, the performance of the HD system is also given to study the impact of the RSI on the FD-SM-MIMO system. Unless otherwise stated, the system parameters are set as follows. The average transmission power $P_{\rm A} = P_{\rm B} = P$. The variance of AWGN $\sigma_{\rm A}^2 = \sigma_{\rm B}^2 = \sigma^2 = 1$. The average SNR is defined as ${\rm SNR} = P/\sigma^2$. The number of selected transmission antennas $S_{\rm A} = S_{\rm B} = S = 2$. The number of transmission antennas $N_{\rm t}^{\rm A} = N_{\rm t}^{\rm B} = N_{\rm t} = 4$ and reception antennas $N_{\rm r}^{\rm A} = N_{\rm r}^{\rm B} = N_{\rm r} = 2$. Since the parameters of two terminals A and B are similar, the OP and SEP of A and B are also similar. Therefore, from now on, we will use the words "the OP and SEP of the FD-SM-MIMO system" to refer to "the OP and SEP of both A or B." The simulation results were obtained using 10^7 channel realizations, which satisfy the Monte-Carlo condition of reliable evaluation.

In Fig. 2, the OP of the FD-SM-MIMO system in the case with TAS is compared with that in the case without TAS. Furthermore, the OP of the FD-SM-MIMO system is also compared with that of the HD-SM-MIMO system. We use $\tilde{\Omega} = -10$ dB, $\mathcal{R} = 2$ bit/s/Hz. The OPs of the considered FD-SM-MIMO system with and without TAS are plotted by using (15) and (21), respectively. It is noted that the OPs of the HD-SM-MIMO system are also plotted by using (15) and (21) by setting $\tilde{\Omega} = 0$. As shown in the figure, the analytical results perfectly match the simulation one, which proves the correctness of Theorem 1. Using TAS, both FD- and HD-MIMO systems can reduce the OP of the system significantly. Particularly, when ${\rm SNR} = 20$ dB, the OP of the FD-SM-MIMO system with TAS is nearly 10^{-4}

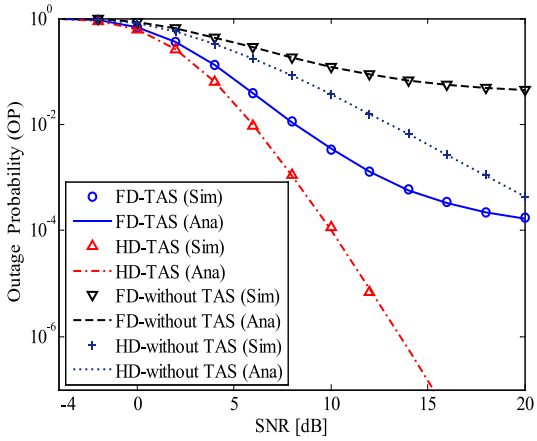

Fig. 2. OPs of the considered FD-SM-MIMO systems with and without TAS versus the average SNR. $\tilde{\Omega} = -10$ dB, $\mathcal{R} = 2$ bit/s/Hz.

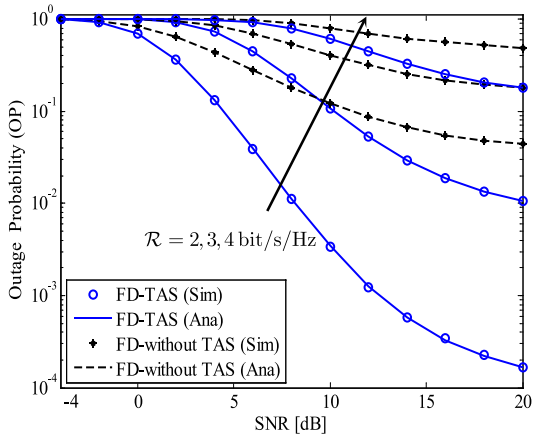

Fig. 3. Impact of data transmission rate $\mathcal{R}$ on the OPs of the FD-SM-MIMO systems with and without TAS. $\tilde{\Omega} = -10$ dB.

while that is only about 4.10^{-2} in the case without TAS. Moreover, the OPs of both FD-SM-MIMO systems with and without TAS suffer from an outage floor due to the impact of the RSI. With the considered RSI ($\tilde{\Omega} = -10$ dB), the OP of FD-SM-MIMO system with TAS reduces to 6.10^{-4} while the OP of HD-SM-MIMO system with TAS attains 10^{-7} for the same ${\rm SNR} = 15$ dB. It is also noted that the OPs of HD-SM-MIMO system with and without TAS in this article are similar to those in [17].

Fig. 3 illustrates the impact of the data transmission rates on the OPs of the FD-SM-MIMO system for three typical values of $\mathcal{R}$, i.e., $\mathcal{R} = 2$, 3, 4 bit/s/Hz. It is obvious that the data transmission rate has strong impact on the OPs of the FD-SM-MIMO system. At low data transmission rate and ${\rm SNR} = 12$ dB, i.e., $\mathcal{R} = 2$ bit/s/Hz, the OP with TAS is 10^{-3} while the OP without TAS is only 10^{-1}. Furthermore, at higher data transmission rate, i.e., $\mathcal{R} = 3$ bit/s/Hz, when ${\rm SNR} = 20$ dB, the OP with TAS reduces to the outage floor of 10^{-2} while it is approximate 10^{-4} at $\mathcal{R} = 2$ bit/s/Hz. When $\mathcal{R}$ increases, such as $\mathcal{R} = 4$ bit/s/Hz, the OPs with and without TAS are significantly higher in comparison with the case of $\mathcal{R} = 2$ bit/s/Hz. Although

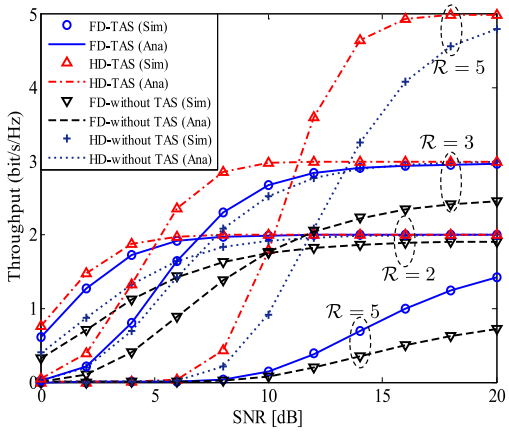

Fig. 4. Throughput of the FD-SM-MIMO and HD-SM-MIMO systems with and without TAS versus the average SNR. $\tilde{\Omega} = -10$ dB.

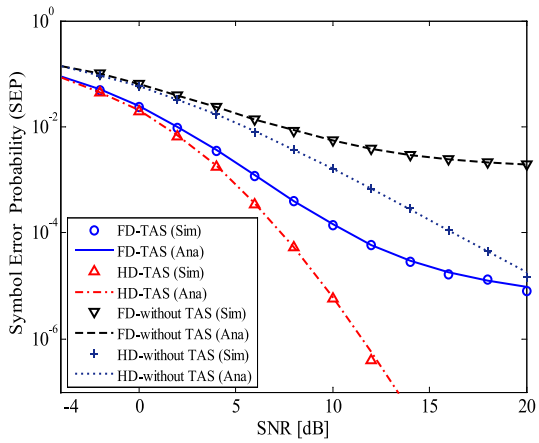

Fig. 5. SEPs of the FD-SM-MIMO systems with and without TAS versus the average SNR using BPSK modulation. $\tilde{\Omega} = -10$ dB.

the TAS scheme can greatly reduce the OP of FD-SM-MIMO system, in the case of high data transmission rate, i.e., $\mathcal{R} = 4$ bit/s/Hz, the OP increases remarkably. Therefore, depending on the requirements of the FD-SM-MIMO system in practical scenarios, we can choose a suitable data transmission rate. For example, when $\text{OP} = 10^{-3}$ is required, we use $\mathcal{R} = 2$ bit/s/Hz and $\text{SNR} = 12$ dB. In contrast, when $\text{OP} = 10^{-2}$, we can use either $\mathcal{R} = 2$ bit/s/Hz and $\text{SNR} = 8$ dB or $\mathcal{R} = 3$ bit/s/Hz and $\text{SNR} = 20$ dB.

Fig. 4 shows the network throughput $\mathcal{T}$ of the FD-SM-MIMO system, which is defined as $\mathcal{T} = \mathcal{R}(1 - \mathcal{P}_{\text{out}})$, and $\mathcal{P}_{\text{out}}$ is given in (15) and (16) for the case with TAS and in (21) and (22) for the case without TAS. As can be seen from Fig. 4, in the case $\mathcal{R} = 2$ bit/s/Hz, the throughput of the FD-SM-MIMO system with TAS is higher than that of the HD-SM-MIMO system without TAS. Moreover, all three systems (FD-SM-MIMO with TAS, HD-SM-MIMO with TAS and without TAS) reach the target throughput $\mathcal{R} = 2$ bit/s/Hz at $\text{SNR} = 10$ dB. Meanwhile, the throughput of the remaining system (FD-SM-MIMO without TAS) is saturated at $\mathcal{T} = 1.9$ bit/s/Hz.

Fig. 5 investigates the SEP of the FD-SM-MIMO system versus the average SNR for the BPSK modulation ($a = 1$ and $b = 2$) and $\tilde{\Omega} = -10$ dB. We use (25) and (28) to plot the SEPs of the FD-SM-MIMO systems with and without TAS, respectively. The SEPs of the HD-SM-MIMO systems with and without TAS are obtained from (25) and (28), respectively, by setting $\tilde{\Omega} = 0$. We can see that all analytical results match well with the simulation ones. Furthermore, the SEP of the FD-SM-MIMO system with TAS is much lower than the case without TAS. Specifically, the SEP with TAS is 10^{-5} while that without TAS is 2.10^{-2} at $\text{SNR} = 20$ dB, which proves the benefit of using TAS scheme in the FD-SM-MIMO system. On the other hand, the SEP of the FD-SM-MIMO system with TAS is always better than the SEP of the HD-SM-MIMO system without TAS when $\text{SNR} \leq 20$ dB. However, at higher transmission power, the SEP of the FD-SM-MIMO system with TAS is worse than that of the HD-SM-MIMO system without TAS due to the influence of the RSI in the FD mode. This feature will be investigated further in the next figure.

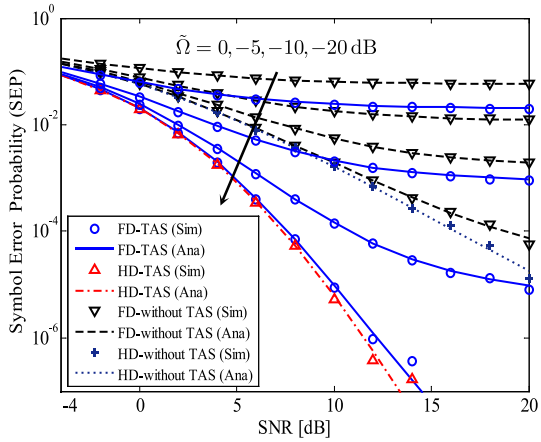

Fig. 6. Impact of the RSI on the SEP of the FD-SM-MIMO systems with and without TAS.

Fig. 6 plots the impact of the RSI on the SEP of the FD-SM-MIMO system for the BPSK modulation. The SIC capability is varied as follows: $\tilde{\Omega} = 0, -5, -10, -20$ dB. Other parameters are similar to those used in Fig. 5. It is obvious that the RSI has a strong impact on the SEP of the FD-SM-MIMO system, especially when the RSI is high. Particularly, when the RSI is very small, i.e., $\tilde{\Omega} = -20$ dB, the SEPs of the FD-SM-MIMO and the HD-SM-MIMO system with TAS are similar for $\text{SNR} < 10$ dB. In the higher SNR regime, such as $\text{SNR} > 10$ dB, the SEP of the FD-SM-MIMO system with TAS is lower than that of HD-SM-MIMO system with TAS. It is because the RSI is expressed as $\sigma^2_{\text{RSI}} = \tilde{\Omega}P$. Thus, higher transmission power results in higher RSI. In the case without TAS, the difference between the SEPs of the FD-SM-MIMO and HD-SM-MIMO systems is significant when $\text{SNR} > 14$ dB. Furthermore, in the case of larger RSI, i.e., $\tilde{\Omega} = 0$ dB or $\tilde{\Omega} = -5$ dB, the SEP of the FD-SM-MIMO system goes to the error floor quickly for both the cases with and without TAS.

Fig. 7 depicts the effect of the number of transmission and reception antennas on the SEPs of the FD-SM-MIMO system. The number of transmission and reception antennas are changed as $N_{\text{t}} = 4$, $N_{\text{t}} = 6$ and $N_{\text{r}} = 2$, $N_{\text{r}} = 4$. As observed

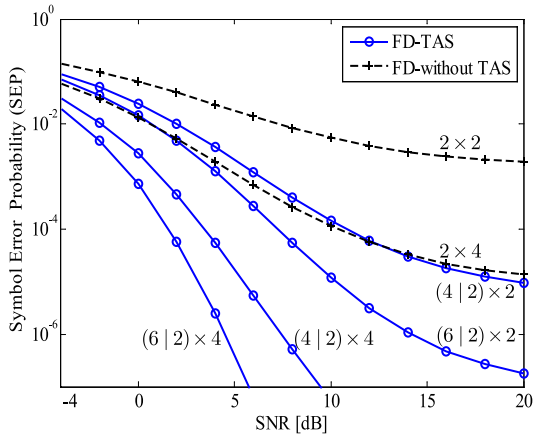

Fig. 7. SEPs of the FD-SM-MIMO system with and without TAS scheme for different numbers of transmission and reception antennas.

from Fig. 7, the SEP is strongly impacted by the number of transmission and reception antennas, especially in the case with TAS. It is noted that the notations in Fig. 7 refer to the numbers of transmission antennas ($N_{\rm t}$), TAS (S), and reception antennas ($N_{\rm r}$). For example, $(6|2) \times 4$ represents $N_{\rm t} = 6$, $S = 2$, and $N_{\rm r} = 4$. In the case without TAS, 2×2 means $N_{\rm t} = 2$ and $N_{\rm r} = 2$. We can see that the SEP of $(4|2) \times 2$ system is similar to that of 2×4 system. For the same SEP $= 10^{-4}$, when the number of transmission antennas increases, i.e., $N_{\rm t} = 6$, the SEP of $(6|2) \times 2$ system has 6 dB gain compared with the SEP of $(4|2) \times 2$ system and the $(4|2) \times 4$ system has a gain about 4 dB compared with the $(6|2) \times 2$ system.

V. Conclusion

In this article, we have analyzed the performance of the FD-SM-MIMO system with TAS. Using theoretical analysis, we have successfully derived the exact closed-form expressions for the OP, network throughput, and SEP of the system. The derived performance expressions not only can be used for evaluating the FD-SM-MIMO system but also the HD-SM-MIMO one by simply setting the RSI equal to zero. Both numerical and simulation results show that using TAS can improve the performance of the FD-SM-MIMO system significantly at the cost of additional employed antennas. In addition, the performance of FD-SM-MIMO system with TAS is also shown to be better than the HD-SM-MIMO system without TAS. Therefore, given available space for installing more antennas, it is recommended that TAS be used to obtain the FD-SM-MIMO performance enhancement.

Appendix A

This appendix gives the detailed derivations of the OP for the considered FD-SM-MIMO system.

In the MIMO system with TAS, a set of sum channel gains, such as Y, are rearranged and, then, S antennas ($S_{\rm A}$ of terminal A and $S_{\rm B}$ of terminal B) are selected to maximize the received power. At terminal B, the PDF of $Y_{w_{\rm A}{\rm B}}$ in the case that $Y_{1{\rm B}} \le Y_{2{\rm B}} \le \cdots \le Y_{w_{\rm A}{\rm B}} \le \cdots \le Y_{N_{\rm t}^{\rm A}{\rm B}}$ can be calculated as follows [37, Eq. 2.1.6]

$$f_{Y_{w_{\rm A}{\rm B}}}(x) = \frac{1}{B(w_{\rm A}, N_{\rm t}^{\rm A} - w_{\rm A} + 1)} \times \left[F_Y(x)\right]^{w_{\rm A}-1} \left[1 - F_Y(x)\right]^{N_{\rm t}^{\rm A}-w_{\rm A}} f_Y(x). \tag{30}$$

Based on (30), the PDF of instantaneous $\|\mathbf{h}_i^{\rm B}\|^2$ is, then, given by [17]

$$f_{\|\mathbf{h}_i^{\rm B}\|^2}(x) = \frac{1}{N_{\rm t}^{\rm A} - w_{\rm A} + 1} \sum_{l=w_{\rm A}}^{N_{\rm t}^{\rm A}} \frac{1}{B(l, N_{\rm t}^{\rm A} - l + 1)} \times \left[F_Y(x)\right]^{l-1} \left[1 - F_Y(x)\right]^{N_{\rm t}^{\rm A}-l} f_Y(x). \tag{31}$$

Replacing $F_Y(x)$ and $f_Y(x)$ in (19) and (20) into (31), we have

$$f_{\|\mathbf{h}_i^{\rm B}\|^2}(x) = \frac{1}{N_{\rm t}^{\rm A} - w_{\rm A} + 1} \sum_{l=w_{\rm A}}^{N_{\rm t}^{\rm A}} \frac{1}{B(l, N_{\rm t}^{\rm A} - l + 1)} \times \left[1 - e^{-x} \sum_{l=0}^{N_{\rm r}^{\rm B}-1} \frac{x^l}{l!}\right]^{l-1} \left[e^{-x} \sum_{l=0}^{N_{\rm r}^{\rm B}-1} \frac{x^l}{l!}\right]^{N_{\rm t}^{\rm A}-l} \times \frac{x^{N_{\rm r}^{\rm B}-1} e^{-x}}{\Gamma(N_{\rm r}^{\rm B})}. \tag{32}$$

Then, applying the finite summation [34], i.e.,

$$\sum_{l=0}^{N_{\rm r}^{\rm B}-1} \frac{x^l}{l!} = e^x \frac{\Gamma(N_{\rm r}^{\rm B}, x)}{\Gamma(N_{\rm r}^{\rm B})}$$

we can rewrite (32) as

$$f_{\|\mathbf{h}_i^{\rm B}\|^2}(x) = \frac{1}{N_{\rm t}^{\rm A} - w_{\rm A} + 1} \sum_{l=w_{\rm A}}^{N_{\rm t}^{\rm A}} \frac{1}{B(l, N_{\rm t}^{\rm A} - l + 1)} \times \left[1 - \frac{\Gamma(N_{\rm r}^{\rm B}, x)}{\Gamma(N_{\rm r}^{\rm B})}\right]^{l-1} \left[\frac{\Gamma(N_{\rm r}^{\rm B}, x)}{\Gamma(N_{\rm r}^{\rm B})}\right]^{N_{\rm t}^{\rm A}-l} \times \frac{x^{N_{\rm r}^{\rm B}-1} e^{-x}}{\Gamma(N_{\rm r}^{\rm B})}. \tag{33}$$

Finally, the OP of terminal B is obtained as follows:

$$\mathcal{P}_{\rm out}^{\rm B} = \Pr\left\{\|\mathbf{h}_i^{\rm B}\|^2 < \frac{\gamma_{\rm th}}{\bar{\gamma}_{\rm B}}\right\} = \int_0^{\frac{\gamma_{\rm th}}{\bar{\gamma}_{\rm B}}} f_{\|\mathbf{h}_i^{\rm B}\|^2}(x) dx = \frac{1}{(N_{\rm t}^{\rm A} - w_{\rm A} + 1)\Gamma(N_{\rm r}^{\rm B})} \sum_{l=w_{\rm A}}^{N_{\rm t}^{\rm A}} \frac{1}{B(l, N_{\rm t}^{\rm A} - l + 1)} \times \int_0^{\frac{\gamma_{\rm th}}{\bar{\gamma}_{\rm B}}} \left[1 - \frac{\Gamma(N_{\rm r}^{\rm B}, x)}{\Gamma(N_{\rm r}^{\rm B})}\right]^{l-1} \left[\frac{\Gamma(N_{\rm r}^{\rm B}, x)}{\Gamma(N_{\rm r}^{\rm B})}\right]^{N_{\rm t}^{\rm A}-l} \times x^{N_{\rm r}^{\rm B}-1} e^{-x} dx. \tag{34}$$

Using the Gaussian–Chebyshev quadrature method [34] for the integral in (34), we have

$$\int_0^{\frac{\gamma_{\rm th}}{\bar{\gamma}_{\rm B}}} \left[1-\frac{\Gamma(N_{\rm r}^{\rm B},x)}{\Gamma(N_{\rm r}^{\rm B})}\right]^{l-1}\left[\frac{\Gamma(N_{\rm r}^{\rm B},x)}{\Gamma(N_{\rm r}^{\rm B})}\right]^{N_{\rm t}^{\rm A}-l} x^{N_{\rm r}^{\rm B}-1}e^{-x}dx$$
$$=\frac{\pi\gamma_{\rm th}}{2M\bar{\gamma}_{\rm B}}\sum_{m=1}^{M}\sqrt{1-\phi_m^2}\left[1-\frac{\Gamma(N_{\rm r}^{\rm B},\chi_{\rm B})}{\Gamma(N_{\rm r}^{\rm B})}\right]^{l-1}$$
$$\times\left[\frac{\Gamma(N_{\rm r}^{\rm B},\chi_{\rm B})}{\Gamma(N_{\rm r}^{\rm B})}\right]^{N_{\rm t}^{\rm A}-l}\chi_{\rm B}^{N_{\rm r}^{\rm B}-1}e^{-\chi_{\rm B}}. \quad (35)$$

Substituting (35) into (34), we obtain the OP of terminal B as in (16) of Theorem 1. The OP of terminal A can be derived in the same ways. The proof is, thus, complete.

APPENDIX B

This appendix provides the detailed derivations of the SEP for the considered FD-SM-MIMO system.

Replacing $\gamma_{\rm th}$ in (16) by x, then $\chi_{\rm B}$ becomes $\chi_{\rm B}=\frac{\gamma_{\rm th}}{2\bar{\gamma}_{\rm B}}(1+\phi_m)=\psi_{\rm B}x$. After that, substituting (16) into (24), the $\mathrm{SEP}_{\rm B}$ is given by

$$\mathrm{SEP}_{\rm B}=\frac{a\sqrt{b}}{2\sqrt{2\pi}}\int_0^{\infty}\frac{e^{-bx/2}}{\sqrt{x}}\frac{\pi x}{2M(N_{\rm t}^{\rm A}-w_{\rm A}+1)\Gamma(N_{\rm r}^{\rm B})\bar{\gamma}_{\rm B}}$$
$$\times\sum_{l=w_{\rm A}}^{N_{\rm t}^{\rm A}}\sum_{m=1}^{M}\frac{\sqrt{1-\phi_m^2}}{B(l,N_{\rm t}^{\rm A}-l+1)}$$
$$\times\left[1-\frac{\Gamma(N_{\rm r}^{\rm B},\psi_{\rm B}x)}{\Gamma(N_{\rm r}^{\rm B})}\right]^{l-1}\left[\frac{\Gamma(N_{\rm r}^{\rm B},\psi_{\rm B}x)}{\Gamma(N_{\rm r}^{\rm B})}\right]^{N_{\rm t}^{\rm A}-l}$$
$$\times(\psi_{\rm B}x)^{N_{\rm r}^{\rm B}-1}e^{-\psi_{\rm B}x}dx. \quad (36)$$

Then, we rewrite (36) as

$$\mathrm{SEP}_{\rm B}=\frac{a\sqrt{b\pi}}{4\sqrt{2}M(N_{\rm t}^{\rm A}-w_{\rm A}+1)\Gamma(N_{\rm r}^{\rm B})\bar{\gamma}_{\rm B}}$$
$$\times\sum_{l=w_{\rm A}}^{N_{\rm t}^{\rm A}}\sum_{m=1}^{M}\frac{\sqrt{1-\phi_m^2}\psi_{\rm B}^{N_{\rm r}^{\rm B}-1}}{B(l,N_{\rm t}^{\rm A}-l+1)}$$
$$\times\int_0^{\infty}\left[1-\frac{\Gamma(N_{\rm r}^{\rm B},\psi_{\rm B}x)}{\Gamma(N_{\rm r}^{\rm B})}\right]^{l-1}\left[\frac{\Gamma(N_{\rm r}^{\rm B},\psi_{\rm B}x)}{\Gamma(N_{\rm r}^{\rm B})}\right]^{N_{\rm t}^{\rm A}-l}$$
$$\times x^{N_{\rm r}^{\rm B}-\frac{1}{2}}e^{-(\psi_{\rm B}+\frac{b}{2})x}dx. \quad (37)$$

Let $z=e^{-(\psi_{\rm B}+\frac{b}{2})x}$, the integral in (37) can be computed as

$$\int_0^{\infty}\left[1-\frac{\Gamma(N_{\rm r}^{\rm B},\psi_{\rm B}x)}{\Gamma(N_{\rm r}^{\rm B})}\right]^{l-1}\left[\frac{\Gamma(N_{\rm r}^{\rm B},\psi_{\rm B}x)}{\Gamma(N_{\rm r}^{\rm B})}\right]^{N_{\rm t}^{\rm A}-l}$$
$$\times x^{N_{\rm r}^{\rm B}-\frac{1}{2}}e^{-(\psi_{\rm B}+\frac{b}{2})x}dx$$
$$=\frac{1}{\psi_{\rm B}+\frac{b}{2}}\int_0^1\left[1-\frac{\Gamma\left(N_{\rm r}^{\rm B},\frac{-\psi_{\rm B}\ln z}{\psi_{\rm B}+\frac{b}{2}}\right)}{\Gamma(N_{\rm r}^{\rm B})}\right]^{l-1}$$
$$\times\left[\frac{\Gamma\left(N_{\rm r}^{\rm B},\frac{-\psi_{\rm B}\ln z}{\psi_{\rm B}+\frac{b}{2}}\right)}{\Gamma(N_{\rm r}^{\rm B})}\right]^{N_{\rm t}^{\rm A}-l}\left(\frac{-\ln z}{\psi_{\rm B}+\frac{b}{2}}\right)^{N_{\rm r}^{\rm B}-\frac{1}{2}}dz. \quad (38)$$

By applying the Gaussian–Chebyshev quadrature method [34], the integral in (38) can be solved. Finally, the exact closed-form expression of $\mathrm{SEP}_{\rm B}$ is obtained as in (26) of Theorem 2. Similarly, we can get the expression of $\mathrm{SEP}_{\rm A}$. The proof is complete.

REFERENCES

[1] N. Jazdi, "Cyber physical systems in the techcontext of industry 4.0," in *Proc. IEEE Int. Conf. Autom., Qual. Testing, Robot.*, 2014, pp. 1–4.

[2] "Future technology trends of terrestrial IMT systems," Tech. Rep., ITU-R Report, M series, 2015.

[3] B. C. Nguyen, T. M. Hoang, and P. T. Tran, "Performance analysis of full-duplex decode-and-forward relay system with energy harvesting over nakagami-m fading channels," *AEU-Int. J. Electron. Commun.*, vol. 98, pp. 114–122, 2019.

[4] S. Hong *et al.*, "Applications of self-interference cancellation in 5g and beyond," *IEEE Commun. Mag.*, vol. 52, no. 2, pp. 114–121, Feb. 2014.

[5] B. C. Nguyen *et al.*, "Performance analysis of vehicle-to-vehicle communication with full-duplex amplify-and-forward relay over double-rayleigh fading channels," *Veh. Commun.*, vol. 19, 2019, Art. no. 100166.

[6] E. Aryafar, M. A. Khojastepour, K. Sundaresan, S. Rangarajan, and M. Chiang, "Midu: Enabling MIMO full duplex," in *Proc. 18th Annu. Int. Conf. Mobile Comput. Netw.*, 2012, pp. 257–268.

[7] D. Bharadia, E. McMilin, and S. Katti, "Full duplex radios," *ACM SIGCOMM Comput. Commun. Rev.*, vol. 43, no. 4, pp. 375–386, 2013.

[8] R. Y. Mesleh, H. Haas, S. Sinanovic, C. W. Ahn, and S. Yun, "Spatial modulation," *IEEE Trans. Veh. Technol.*, vol. 57, no. 4, pp. 2228–2241, Jul. 2008.

[9] M. Di Renzo, H. Haas, A. Ghrayeb, S. Sugiura, and L. Hanzo, "Spatial modulation for generalized MIMO: Challenges, opportunities, and implementation," *Proc. IEEE*, vol. 102, no. 1, pp. 56–103, Jan. 2013.

[10] E. Basar, U. Aygolu, E. Panayirci, and H. V. Poor, "Space-time block coded spatial modulation," *IEEE Trans. Commun.*, vol. 59, no. 3, pp. 823–832, Mar. 2011.

[11] M.-T. Le, V.-D. Ngo, H.-A. Mai, X. N. Tran, and M. Di Renzo, "Spatially modulated orthogonal space-time block codes with non-vanishing determinants," *IEEE Trans. Commun.*, vol. 62, no. 1, pp. 85–99, Jan. 2014.

[12] M. Di Renzo and H. Haas, "On transmit diversity for spatial modulation mimo: Impact of spatial constellation diagram and shaping filters at the transmitter," *IEEE Trans. Veh. Technol.*, vol. 62, no. 6, pp. 2507–2531, Jul. 2013.

[13] X. Li and L. Wang, "High rate space-time block coded spatial modulation with cyclic structure," *IEEE Commun. Lett.*, vol. 18, no. 4, pp. 532–535, Apr. 2014.

[14] X. N. Tran, X.-N. Nguyen, M.-T. Le, and V.-D. Ngo, "High-rate spatially modulated space time block code," *IEEE Commun. Lett.*, vol. 22, no. 12, pp. 2595–2598, Dec. 2018.

[15] R. Rajashekar, K. Hari, and L. Hanzo, "Antenna selection in spatial modulation systems," *IEEE Commun. Lett.*, vol. 17, no. 3, pp. 521–524, Mar. 2013.

[16] K. Ntontin, M. Di Renzo, A. I. Pérez-Neira, and C. Verikoukis, "A low-complexity method for antenna selection in spatial modulation systems," *IEEE Commun. Lett.*, vol. 17, no. 12, pp. 2312–2315, Dec. 2013.

[17] B. Kumbhani and R. Kshetrimayum, "Outage probability analysis of spatial modulation systems with antenna selection," *Electron. Lett.*, vol. 50, no. 2, pp. 125–126, 2014.

[18] F. Yarkın and I. Altunbas, "Outage performance of spatial modulation with transmit antenna selection over Nakagami-m fading channels with arbitrary m," in *Proc. IEEE 8th Int. Congr. Ultra Modern Telecommun. Control Syst. Workshops*, 2016, pp. 438–442.

[19] B. Jiao, M. Wen, M. Ma, and H. V. Poor, "Spatial modulated full duplex," *IEEE Wireless Commun. Lett.*, vol. 3, no. 6, pp. 641–644, Dec. 2014.

[20] A. Koc, I. Altunbas, and E. Basar, "Two-way full-duplex spatial modulation systems with wireless powered AF relaying," *IEEE Wireless Commun. Lett.*, vol. 7, no. 3, pp. 444–447, Jun. 2018.

[21] S. Narayanan, H. Ahmadi, and M. F. Flanagan, "On the performance of spatial modulation MIMO for full-duplex relay networks," *IEEE Trans. Wireless Commun.*, vol. 16, no. 6, pp. 3727–3746, Jun. 2017.

[22] P. Raviteja, Y. Hong, and E. Viterbo, "Spatial modulation in full-duplex relaying," *IEEE Commun. Lett.*, vol. 20, no. 10, pp. 2111–2114, Oct. 2016.

[23] J. Zhang, Q. Li, K. J. Kim, Y. Wang, X. Ge, and J. Zhang, "On the performance of full-duplex two-way relay channels with spatial modulation," *IEEE Trans. Commun.*, vol. 64, no. 12, pp. 4966–4982, Dec. 2016.
[24] T. Riihonen, S. Werner, and R. Wichman, "Mitigation of loopback self-interference in full-duplex MIMO relays," *IEEE Trans. Signal Process.*, vol. 59, no. 12, pp. 5983–5993, Dec. 2011.
[25] X. N. Tran, B. C. Nguyen, and D. T. Tran, "Outage probability of two-way full-duplex relay system with hardware impairments," in *Proc. IEEE 3rd Int. Conf. Recent Advances Signal Process., Telecommun. Comput.*, 2019, pp. 135–139.
[26] C. Li, Z. Chen, Y. Wang, Y. Yao, and B. Xia, "Outage analysis of the full-duplex decode-and-forward two-way relay system," *IEEE Trans. Veh. Technol.*, vol. 66, no. 5, pp. 4073–4086, May 2017.
[27] B. C. Nguyen *et al.*, "Performance analysis of full-duplex vehicle-to-vehicle relay system over double-rayleigh fading channels," *Mobile Netw. Appl.*, pp. 1–10, 2019.
[28] B. C. Nguyen and X. N. Tran, "Performance analysis of full-duplex amplify-and-forward relay system with hardware impairments and imperfect self-interference cancellation," *Wireless Commun. Mobile Comput.*, vol. 2019, 2019, Art. no. 4946298.
[29] B. C. Nguyen, X. N. Tran, and D. T. Tran, "Performance analysis of in-band full-duplex amplify-and-forward relay system with direct link," in *Proc. 2nd Int. Conf. Recent Adv. Signal Process., Telecommun. Comput.*, 2018, pp. 192–197.
[30] A. Bhowal and R. S. Kshetrimayum, "Outage probability bound of decode and forward two-way full-duplex relay employing spatial modulation over cascaded α- μ channels," *Int. J. Commun. Syst.*, vol. 32, no. 3, 2019, Art. no. e3876.
[31] A. Bhowal and R. S. Kshetrimayum, "Outage probability bound of decode and forward two-way relay employing optical spatial modulation over gamma-gamma channels," *IET Optoelectronics*, vol. 13, no. 4, pp. 183–190, Aug. 2019.
[32] R. Rajashekar, K. Hari, and L. Hanzo, "Antenna selection in spatial modulation systems," *IEEE Commun. Lett.*, vol. 17, no. 3, pp. 521–524, Mar. 2013.
[33] A. Jeffrey and D. Zwillinger, *Table of Integrals, Series, and Products*. San Francisco, CA, USA: Academic, 2007.
[34] M. Abramowitz and I. A. Stegun, *Handbook of Mathematical Functions with Formulas, Graphs, and Mathematical Tables*, vol. 9. New York, NY, USA: Dover, 1972.
[35] A. Goldsmith, *Wireless Communications*. Cambridge, U.K.: Cambridge Univ. Press, 2005.
[36] H. A. David and H. N. Nagaraja, *Order Statistics*. Hoboken, NJ, USA: Wiley, 2004.

Le Van Nguyen was born in Vinh Phuc, Vietnam, in 1985. She received the B.E. degree in electronic and telecommunication engineering in 2008, and the M.E. degree in electronics engineering in 2010, both from Le Quy Don Technical University, Hanoi, Vietnam. Since October 2015, she has been working toward the Ph.D. degree with Le Quy Don Technical University.

Her current research interests include MIMO, spatial modulation, and signal processing for wireless communication systems.

Ba Cao Nguyen was born in Nghe An, Vietnam. He received the B.S. degree in 2006 from Telecommunication University, Nha Trang, Vietnam, and the M.S. degree in 2011 from the Posts and Telecommunications Institute of Technology (VNPT), Ho Chi Minh City, Vietnam. He received the Ph.D. degree from Le Quy Don Technical University, Hanoi, Vietnam.

He is currently a Lecturer with Telecommunications University, Nhatrang, Vietnam. His research interests include energy harvesting, full-duplex, and cooperative communication.

Xuan Nam Tran (M'03) received the Master's of Engineering degree in telecommunications engineering from the University of Technology Sydney, Ultimo, NSW, Australia, in 1998, and Doctor of Engineering degree in electronic engineering from The University of Electro-Communications, Chofu, Japan, in 2003.

From November 2003 to March 2006, he was a Research Associate with the Information and Communication Systems Group, Department of Information and Communication Engineering, The University of Electro-Communications, Tokyo, Japan. He is currently a Professor with the Department of Communications Engineering, Le Quy Don Technical University, Hanoi, Vietnam. His research interests include the areas of adaptive antennas, space-time processing, space-time coding, and MIMO systems.

Dr. Tran received the 2003 IEEE AP-S Japan Chapter Young Engineer Award. He is a member of IEICE and the Radio-Electronics Association of Vietnam.

Le The Dung (S'14–M'16) received the B.S. degree in electronics and telecommunication engineering from the Ho Chi Minh City University of Technology, Ho Chi Minh City, Vietnam, in 2008, and both the M.S. and Ph.D. degrees in electronics and computer engineering from Hongik University, Seoul, South Korea, in 2012 and 2016, respectively.

From 2007 to 2010, he joined Signet Design Solutions Vietnam as a Hardware Design Engineer. He has been with Chungbuk National University as a Postdoctoral Research Fellow from May 2016. He has more than 50 papers in referred international journals and conferences. His major research interests include routing protocols, network coding, network stability analysis and optimization in mobile ad-hoc networks, cognitive radio ad-hoc networks, and visible light communication networks.

Dr. Dung received the IEEE IS3C2016 Best Paper Award.